

Dependence of overlap topological charge density on Wilson mass parameter*

Zhen Cheng(程贞)[†] Jian-bo Zhang(张剑波)[‡]

Department of Physics, Zhejiang University, Zhejiang 310027, China

Abstract: In this paper, we analyze the dependence of the topological charge density from the overlap operator on the Wilson mass parameter in the overlap kernel by the symmetric multi-probing source (SMP) method. We observe that non-trivial topological objects are removed as the Wilson mass is increased. A comparison of topological charge density calculated by the SMP method using the fermionic definition with that of the gluonic definition by the Wilson flow method is shown. A matching procedure for these two methods is used. We find that there is a best match for topological charge density between the gluonic definition with varied Wilson flow time and the fermionic definition with varied Wilson mass. By using the matching procedure, the proper flow time of Wilson flow in the calculation of topological charge density can be estimated. As the lattice spacing a decreases, the proper flow time also decreases, as expected.

Keywords: lattice QCD, topological charge density, overlap fermion, Wilson flow, SMP method

DOI: 10.1088/1674-1137/abf827

I. INTRODUCTION

Topological charge Q and its density $q(x)$ play an important role in the study of the non-trivial topological structure of QCD vacuum. Topological properties have important phenomenological implications, such as θ dependence and spontaneous chiral symmetry breaking. The confinement may also be related to nontrivial topological properties [1-3]. The topology of QCD gauge fields is a non-perturbative issue; therefore, the lattice method is a good choice to investigate it from first principles. Lattice QCD is powerful for studying the topological structure of the vacuum. There are many definitions of the topological charge for a lattice gauge field [4-6]. These definitions can be characterized either as gluonic or fermionic. In the fermionic definition, topological charge Q is the number of zero modes of the Dirac operator [7, 8]. In contrast, topological charge can be given by the field strength tensor (gluonic definition) on the lattice, and this definition approaches the fermionic definition in the limit $a \rightarrow 0$ [9-11].

The overlap Dirac operator is a solution of the Ginsparg-Wilson equation [12, 13], and the topological charge defined from the overlap fermion will be an exact integer. In the traditional method, the point source is used

in the calculation of topological charge density [14, 15], which makes the computation on the large lattice almost impossible. To reduce the computational cost, the symmetric multi-probing source (SMP) method is introduced to calculate the topological charge density [16]. As the Wilson mass parameter m varies, the value of Q may change [17-20]. The topological charge density $q(x)$ has a strong correlation with the low-lying modes of the Dirac operator, which strongly influences how quarks propagate through the vacuum. Therefore, the topological charge density $q(x)$ is a useful probe of the gauge field. We visualize the topological charge density and view the detailed extra information [21]. In contrast, the topological charge cannot show the details of the QCD vacuum. Therefore, we will focus on the topological charge density $q(x)$ in the study of the topological properties of the QCD vacuum. We show an analysis of the topological charge $q(x)$, obtained using the fermionic definition with different values of m and the gluonic definition with different Wilson flow time. Unlike in the case of Ref. [22], which studied just one time slice, we consider all time slices and show more details on the topological charge density with different topological charge. By analyzing the topological charge density $q(x)$, we can obtain a great amount of in-

Received 7 March 2021; Accepted 15 April 2021; Published online 20 May 2021

* Supported by the National Natural Science Foundation of China (NSFC) (11335001)

[†] E-mail: zjuercz@zju.edu.cn

[‡] E-mail: jbzhang08@zju.edu.cn



Content from this work may be used under the terms of the Creative Commons Attribution 3.0 licence. Any further distribution of this work must maintain attribution to the author(s) and the title of the work, journal citation and DOI. Article funded by SCOAP³ and published under licence by Chinese Physical Society and the Institute of High Energy Physics of the Chinese Academy of Sciences and the Institute of Modern Physics of the Chinese Academy of Sciences and IOP Publishing Ltd

formation about the underlying topological structure. We show a comparison with the gluonic topological charge density that is calculated after the application of the Wilson flow method. This comparison is shown by calculating the matching parameter Ξ_{AB} , which is defined later. Ξ_{AB} is used to measure the match of the topological charge density between the fermionic and gluonic definitions. The best match is found when the matching parameter is nearest to 1. The proper flow time of Wilson flow in the gluonic definition can also be obtained by analyzing the matching procedure. The behavior of the proper flow time toward the continuum limit is also discussed.

II. SIMULATION DETAILS

The pure gauge lattice configurations were generated using a tadpole improved, plaquette plus rectangle gauge action through pseudo-heat-bath algorithm [23, 24]. This gauge action at tree-level $O(a^2)$ -improved is defined as

$$S_G = \frac{5\beta}{3} \sum_{\substack{\mu\nu \\ \nu>\mu}} \text{ReTr}[1 - P_{\mu\nu}(x)] - \frac{\beta}{12u_0^2} \sum_{\substack{\mu\nu \\ \nu>\mu}} \text{ReTr}[1 - R_{\mu\nu}(x)], \quad (1)$$

where $P_{\mu\nu}$ is the plaquette term. The link product $R_{\mu\nu}(x)$ denotes the rectangular 1×2 and 2×1 loops. The mean link u_0 is the tadpole improvement factor that largely corrects for the quantum renormalization of the coefficient for the rectangles relative to the plaquette. u_0 is given by

$$u_0 = \left(\frac{1}{3} \text{ReTr} \langle P_{\mu\nu}(x) \rangle \right)^{1/4}. \quad (2)$$

In the fermionic definitions, we use the overlap operator to calculate topological charge density. The massless overlap Dirac operator is given by [20]

$$D_{\text{ov}} = \left(\mathbb{1} + \frac{D_W}{\sqrt{D_W^\dagger D_W}} \right), \quad (3)$$

where D_W is the Wilson Dirac operator,

$$D_W = \delta_{a,b} \delta_{\alpha,\beta} \delta_{i,j} - \kappa \sum_{\mu=1}^4 \left[(\mathbb{1} - \gamma_\mu)_{\alpha\beta} U_\mu(i)_{ab} \delta_{i,j-\hat{\mu}} + (\mathbb{1} + \gamma_\mu)_{\alpha\beta} U_\mu^\dagger(i-\hat{\mu})_{ab} \delta_{i,j+\hat{\mu}} \right], \quad (4)$$

and κ is the hopping parameter,

$$\kappa = \frac{1}{2(-m+4)}. \quad (5)$$

In the overlap formalism, κ has to be in the range $(\kappa_c, 0.25)$ for D_{ov} to describe a single massless Dirac fermion, and κ_c is the critical value of κ at which the pion mass extrapolates to zero in the simulation with ordinary Wilson fermions. We call m in Eq. (5) the Wilson mass parameter. In this work, we choose parameter κ as the input parameter.

The overlap topological charge density can be calculated as follows:

$$q_{\text{ov}}(x) = \frac{1}{2} \text{Tr}_{c,d} (\gamma_5 D_{\text{ov}}(x)) = \text{Tr}_{c,d} (\tilde{D}_{\text{ov}}(x)), \quad (6)$$

where the trace is over the color and Dirac indices. It is well known that the traditional way of computing $q_{\text{ov}}(x)$ with a point source is almost impossible for a large lattice volume.

To avoid the high computational effort in the calculation of the $q(x)$ with a point source, we apply the SMP method to calculate $q(x)$ [16, 25],

$$\begin{aligned} q_{\text{smp}}(x) &= \sum_{\alpha,a} \psi(x, \alpha, a) (\tilde{D}_{\text{ov}}(x)) \phi_P(S(x, P), \alpha, a) \\ &= \sum_{\alpha,a} \psi(x, \alpha, a) (\tilde{D}_{\text{ov}}(x)) \psi(x, \alpha, a) \\ &\quad + \sum_{\substack{y \neq x \\ y \in S(x, P)}} \psi(x, \alpha, a) (\tilde{D}_{\text{ov}}(x)) \psi(y, \alpha, a) \\ &\approx \sum_{\alpha,a} \psi(x, \alpha, a) (\tilde{D}_{\text{ov}}(x)) \psi(x, \alpha, a), \end{aligned} \quad (7)$$

where x is the seed site at site (x_1, x_2, x_3, x_4) , and y represents the other lattice sites belonging to the set $S(x, P)$. $\phi_P(S(x, P), \alpha, a)$ is the SMP source vector, and ψ is the normalized point source vector. $S(x, P)$ represents the sites with the same color of x obtained by the symmetric coloring scheme $P\left(\frac{n_s}{d}, \frac{n_s}{d}, \frac{n_s}{d}, \frac{n_t}{d}, \text{mode}\right)$. n_s and n_t are the spatial and temporal sizes of the lattice, d is the minimal distance of the coloring scheme, $\text{mode} = 0, 1, 2$ corresponds to the Normal, Split, and Combined mode for scheme P , and the number of SMP sources that cover all lattice sites are $12d^4$, $24d^4$, and $6d^4$, respectively. The term in the third line of Eq. (7) is the summation of space-time off-diagonal elements of $\tilde{D}_{\text{ov}}(x)$. Because of the space-time locality of D_{ov} , this term can be regarded as the error in the calculation of topological charge density. If we choose the proper scheme P of the SMP source, we can neglect the error term and obtain the last line in Eq. (7).

However, the number of normalized point sources is $12N_L$, and $N_L = N_x N_y N_z N_t$ is the lattice volume. This

shows that the SMP method is much cheaper than the point source method in the calculation of topological charge density with the fermionic definition, especially for a large lattice volume. The topological charge using the SMP method is denoted as Q_{smp} , given by

$$Q_{\text{smp}} = \sum_x q_{\text{smp}}(x). \quad (8)$$

Gradient flow is a non-perturbative smoothing procedure, which has been proven to have well-defined numerical and perturbative properties. The gradient flow is defined as the solution of the evolution equations [6, 26-28]

$$\dot{V}_\mu(x, \tau) = -g_0^2 \left[\partial_{x,\mu} S_G(V(\tau)) \right] V_\mu(x, \tau), \quad V_\mu(x, 0) = U_\mu(x), \quad (9)$$

where τ is the dimensionless gradient flow time (Wilson flow time in this work), and $g_0^2 \partial_{x,\mu} S_G(U)$ is given by

$$g_0^2 \partial_{x,\mu} S_G(U) = 2i \sum_a T^a \text{Im Tr} [T^a \Omega_\mu] = \frac{1}{2} (\Omega_\mu(x) - \Omega_\mu^\dagger) - \frac{1}{6} \text{Tr} (\Omega_\mu(x) - \Omega_\mu^\dagger), \quad (10)$$

where T^a ($a = 1, 2, \dots, 8$) are the Hermitian generators of the SU(3) group. $\Omega_\mu = U_\mu(x) X_\mu^\dagger(x)$, and $X_\mu(x)$ represents the so-called staples.

In practice, the gradient flow moves the gauge configuration along the steepest descent direction in the configuration space, such as along the gradient of the action. The chosen sign in the evolution equations leads to a minimization of the action, which is as expected. We use the third order Runge-Kutta method to obtain the solution of the flow in Eq. (9). The gluonic definition of topological charge density in Euclidean spacetime is defined as

$$q(x) = \frac{1}{32\pi^2} \epsilon_{\mu\nu\rho\sigma} \text{Tr} [F_{\mu\nu} F_{\rho\sigma}], \quad (11)$$

with $F_{\mu\nu}$ the gluonic field strength tensor. The topological charge of a gauge field is the four-dimensional integral over space-time of the topological charge density,

$$Q = \int d^4x q(x). \quad (12)$$

The most common definition of the topological charge density in lattice discretization is the clover definition, given by

$$q_L^{\text{clov}}(x) = \frac{1}{32\pi^2} \epsilon_{\mu\nu\rho\sigma} \text{Tr} [C_{\mu\nu}^{\text{clov}} C_{\rho\sigma}^{\text{clov}}], \quad (13)$$

where $C_{\mu\nu}^{\text{clov}}$ is the usual clover leaf.

The field strength tensor $F_{\mu\nu}$ used in this work is three-loop $\mathcal{O}(a^4)$ -improved and defined as [29]

$$F_{\mu\nu}^{\text{Imp}} = \frac{27}{18} C^{(1,1)} - \frac{27}{180} C^{(2,2)} + \frac{1}{90} C^{(3,3)}, \quad (14)$$

where $C^{(m,n)}$ denotes the three $m \times n$ loops used to construct the clover term, and $C^{(1,1)}$ is the clover leaf mentioned above.

The $q(x)$ calculated after Wilson flow to the gauge configuration is denoted as $q_{\text{wf}}(x)$. The topological charge obtained by Wilson flow is denoted as Q_{wf} , given by

$$Q_{\text{wf}} = \sum_x q_{\text{wf}}(x). \quad (15)$$

To fairly compare the two definitions for the topological charge density with the varied Wilson mass parameter, we calculate the matching parameter Ξ_{AB} , given by [30]

$$\Xi_{AB} = \frac{\chi_{AB}^2}{\chi_{AA}\chi_{BB}}, \quad (16)$$

with

$$\chi_{AB} = \frac{1}{V} \sum_x (q_A(x) - \bar{q}_A)(q_B(x) - \bar{q}_B), \quad (17)$$

where \bar{q} denotes the mean value of $q(x)$, and in this work, $q_A(x) \equiv q_{\text{smp}}(x)$, $q_B(x) \equiv q_{\text{wf}}(x)$. When the Ξ_{AB} is nearest to 1, the best match is found [22]. When the best match is reached, the flow time τ is called the proper flow time of Wilson flow, denoted as τ_{pr} . In this work, the step length for numerical integration of Wilson flow is $\delta\tau = 0.005$.

We also calculate the factor Z_{calc} , defined as

$$Z_{\text{calc}} \equiv \frac{\sum_x |q_{\text{ov}}(x)|}{\sum_x |q_{\text{wf}}(x)|}. \quad (18)$$

Because the topological charge of gluonic definition is not always an integer, Z_{calc} is needed in the visualization of the matching procedure. The matching parameter Ξ_{AB} is independent of the value of Z_{calc} .

We will analyze $q(x)$ of all time slices on lattices of 16^4 , $24^3 \times 48$ and 32^4 at the inverse coupling, $\beta = 4.50$,

$\beta = 4.80$, and $\beta = 5.0$, corresponding to the lattice spacing $a = 0.1289$, 0.0845 and 0.0655 fm, respectively. In this work, we calculate the topological charge density of two configurations for lattice volumes 16^4 and $24^4 \times 48$, and one configuration for 32^4 . We show the visualization of the topological charge density and apply the matching procedure to obtain the proper flow time of Wilson flow in the calculation of topological charge density.

III. $q(x)$ FOR DIFFERENT METHODS

Before we proceed with the analysis, we first demonstrate that the SMP method with proper d is a good method to calculate the topological charge density with an overlap Dirac operator. When the source in the calculation of topological charge is a point source, $q_{ps}(x)$ is an exact result of $q_{ov}(x)$. It is reasonable to use $q_{ps}(x)$ as a benchmark for comparison. Due to the high computational cost, we only make a comparison of the point source and the SMP source in Eq. (6) on a $12^3 \times 24$ lattice with $\beta = 4.8$, $\kappa = 0.21$. We show $q_{ps}(x)$ obtained using the point source method and $q_{smp}(x)$ using the SMP method with $d = 6$ in Fig. 1. To show the visualization more clearly, we use a cutoff method, shown as the color map. The same cutoff procedure is used in other visualized figures. It shows that $q_{smp}(x)$ is highly matched with $q_{ps}(x)$. The matching parameter Ξ_{AB} for these two methods is 0.9997 , and we can barely see the difference with the naked eye. This shows that the error caused by the space-time off-diagonal elements of D_{ov} is indeed very small when the distance parameter d of SMP source is proper. Thus, the SMP method is a good choice to calculate the topological charge density while the parameter d is large enough. It is expected that a better match corresponds to a larger distance d [16].

To obtain more precise topological charge density, we choose the distance parameter $d = 8$ in the SMP method on 16^4 , $24^3 \times 48$, and 32^4 ensembles. The results are summarized in Tables 1-5. We only show the visualization of topological charge density $q(x)$ for lattice volume $24^3 \times 48$ at $\beta = 4.80$ as an example. The results for other lattice ensembles are similar. In these calculations of $q(x)$ with $d = 8$ by the SMP method, we find that the topological charge Q_{smp} is very close to an integer and it is not always the same for the same ensemble with different κ values. This is acceptable as zero crossings in the spectral flow of the $\tilde{D}_{ov}(x)$ occur for different κ on the lattice [6, 18]. From the tables, it also shows that Q_{smp} is very sensitive to κ on the coarsest lattice. Q_{smp} changes a little on the finer lattice, and is stable versus the change of κ on the finest lattice. This sensitivity is probably the effect of finite lattice space a . All results indicate that even though the topological charge Q_{smp} from overlap fermions is always an integer, its value is not unique, and it depends on the Wilson mass parameter m .

The SMP topological charge density for three choices κ compared with the proper flow time of Wilson flow τ_{pr} for time slice $t = 24$ as an example is shown in Fig. 2, and $q_{wf}(x)$ is renormalized using Z_{calc} . Other time slices have a similar property. This shows that more Wilson flow time for $q_{wf}(x)$ is needed to match the topological charge density $q_{smp}(x)$ with a smaller κ or larger mass m . This phenomenon may be a result of the smaller κ showing sparser small eigenvalues of D_{ov} , which has a similar effect of smoothing the configurations. However, the detailed reasons need further study. This indicates that the overlap Dirac operator is less sensitive to small objects as κ is decreased, and these objects can be removed by Wilson flow smoothing.

τ_{pr} , Z_{calc} , Ξ_{AB} , Q_{smp} and Q_{wf} of different ensembles

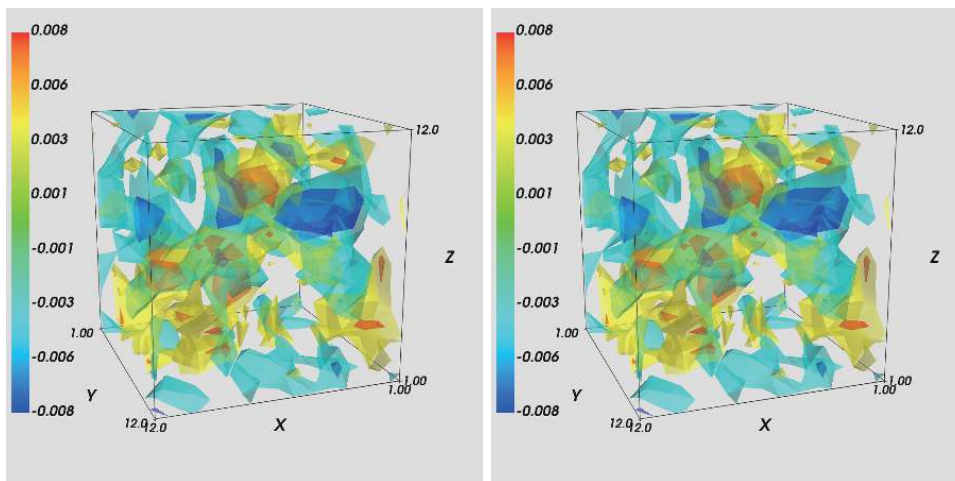


Fig. 1. (color online) $q_{ps}(x)$ and $q_{smp}(x)$ on lattice $12^3 \times 24$ by the point source and SMP source for the $t = 12$ slice; other time slices are similar. To the naked eye, they are almost the same. The parameters $\kappa = 0.21$ and $\beta = 4.80$ are the same for both setups. In the figures, we use a color cutoff method shown as the color map. (left): Point source, (right): SMP source.

Table 1. Proper time of Wilson flow τ_{pr} needed to match the SMP topological charge density with different κ at $\beta = 4.50$ and lattice volume 16^4 for conf. 1. Q_{smp} is obtained by the SMP method, and Q_{wf} is the result of Wilson flow with τ_{pr} .

κ	τ_{pr}	Z_{calc}	Ξ_{AB}	Q_{smp}	Q_{wf}
0.17	0.360	0.5121	0.6853	5.0010	3.5420
0.18	0.365	0.7351	0.7259	5.0015	3.5299
0.19	0.350	0.8656	0.7309	6.0005	3.5847
0.21	0.330	1.0045	0.7267	3.9990	3.6378
0.23	0.320	1.0073	0.7030	1.9963	3.6796

Table 2. Proper time of Wilson flow τ_{pr} needed to match the SMP topological charge density with different κ at $\beta = 4.50$ and lattice volume 16^4 for conf. 2. Q_{smp} is obtained by the SMP method, and Q_{wf} is the result of Wilson flow with τ_{pr} .

κ	τ_{pr}	Z_{calc}	Ξ_{AB}	Q_{smp}	Q_{wf}
0.17	0.365	0.5230	0.7006	-6.0091	-7.2945
0.18	0.360	0.7235	0.7339	-6.0052	-7.3027
0.19	0.350	0.8680	0.7471	-5.0026	-7.3181
0.21	0.330	1.0077	0.7322	-3.9997	-7.3458
0.23	0.320	1.0121	0.7096	-5.9964	-7.3581

Table 3. Proper time of Wilson flow τ_{pr} needed to match the SMP topological charge density with different κ at $\beta = 4.80$ and lattice volume $24^3 \times 48$ for conf. 1. Q_{smp} is obtained by the SMP method, and Q_{wf} is the result of Wilson flow with τ_{pr} .

κ	τ_{pr}	Z_{calc}	Ξ_{AB}	Q_{smp}	Q_{wf}
0.17	0.365	0.6811	0.7653	8.0077	8.5997
0.18	0.345	0.8364	0.7670	7.0078	8.6863
0.19	0.325	0.9275	0.7580	7.0095	8.7954
0.21	0.305	1.0215	0.7324	9.0169	8.9322
0.23	0.295	0.9811	0.6972	9.0279	9.0130

Table 4. Proper time of Wilson flow τ_{pr} needed to match the SMP topological charge density with varied κ at $\beta = 4.80$ and lattice volume $24^3 \times 48$ for conf. 2. Q_{smp} is obtained by the SMP method, and Q_{wf} is the result of Wilson flow with τ_{pr} .

κ	τ_{pr}	Z_{calc}	Ξ_{AB}	Q_{smp}	Q_{wf}
0.17	0.365	0.6802	0.7661	4.9938	4.3224
0.18	0.345	0.8359	0.7656	4.9932	4.3289
0.19	0.325	0.9274	0.7574	3.9942	4.3365
0.21	0.305	1.0211	0.7309	3.9949	4.3431
0.23	0.290	0.9596	0.6953	3.9967	4.3454

Table 5. Proper time of Wilson flow τ_{pr} needed to match the SMP topological charge density with varied κ at $\beta = 5.0$ and lattice volume 32^4 . Q_{smp} is obtained by the SMP method, and Q_{wf} is the result of Wilson flow with τ_{pr} .

κ	τ_{pr}	Z_{calc}	Ξ_{AB}	Q_{smp}	Q_{wf}
0.17	0.355	0.7271	0.7678	3.0099	2.8066
0.18	0.335	0.8724	0.7627	3.0059	2.7340
0.19	0.315	0.9507	0.7515	3.0069	2.6380
0.21	0.295	1.0233	0.7222	3.0127	2.5120
0.23	0.285	0.9636	0.6818	3.0240	2.4352

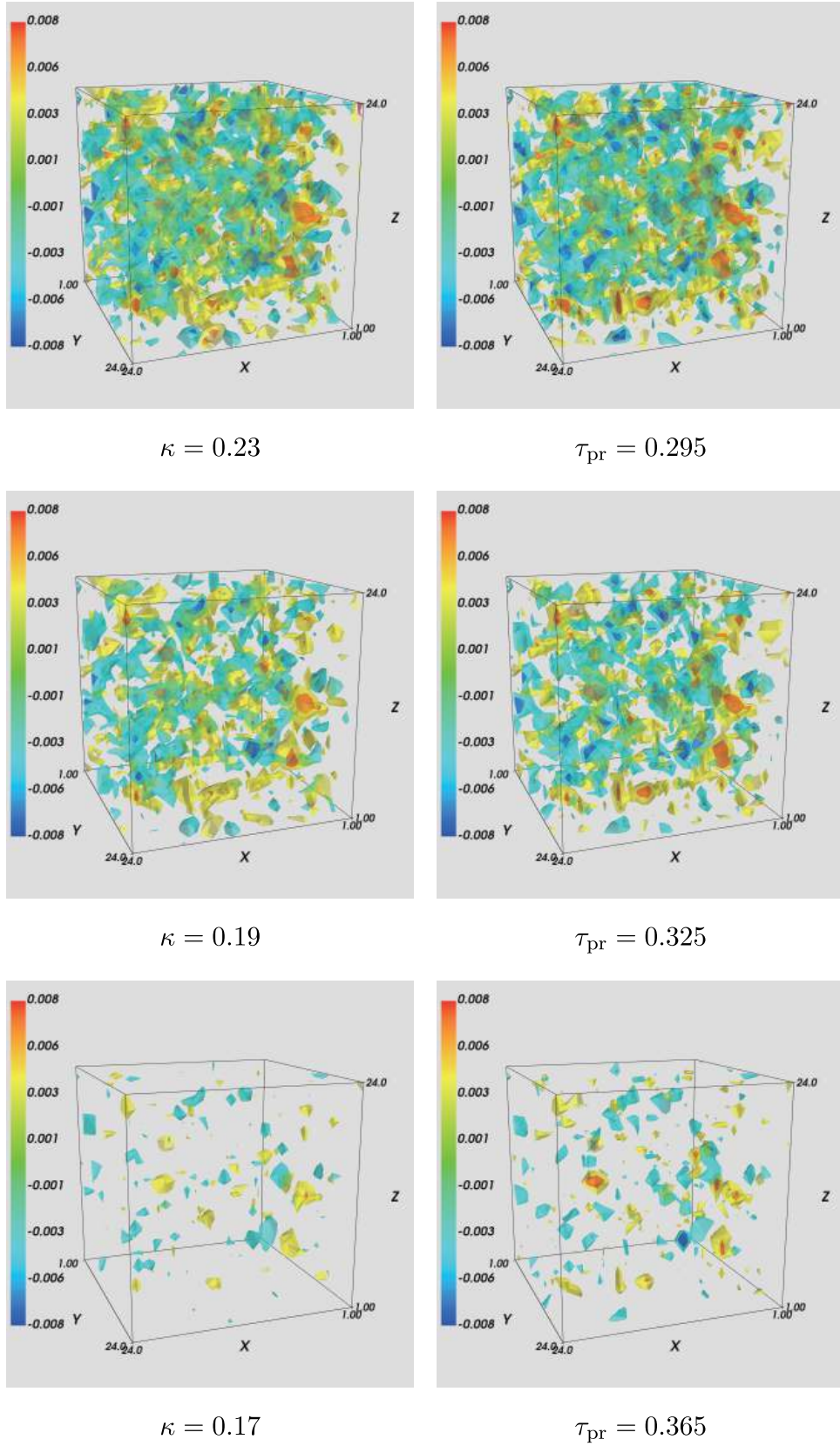


Fig. 2. (color online) Best matched topological charge density $q_{\text{wf}}(x)$ (right) calculated by the Wilson flow method compared with the overlap $q_{\text{smp}}(x)$ for the time slice $t=24$, where $q_{\text{wf}}(x)$ is renormalized using Z_{calc} . τ_{pr} is the proper flow time of Wilson flow fixed by a matching procedure. A color cutoff method is used shown as the color map in the figures.

for five different κ are shown in Tables 1-5, respectively. When calculating Z_{calc} , the flow time of Wilson flow is τ_{pr} . As the parameter κ increases, there is a monotonically decreasing trend in the proper flow time of Wilson flow in all tables. This shows that the matching procedure is effective and the proper flow time of Wilson flow is almost equal at the same κ for different configurations of the same lattice ensembles. When the parameter κ is fixed, Ξ_{AB} and Z_{calc} are independent of topological charge Q and very close for different configurations with the same lattice volume. The value of Ξ_{AB} is approximately in the range [0.68,0.77]. We can see that the proper flow time of Wilson flow τ_{pr} is different for different κ . However, it is reasonable to choose the average value of the proper flow time of Wilson flow of different κ as the proper $\bar{\tau}_{\text{pr}}$. This is approximately $\bar{\tau}_{\text{pr}} = 0.345$, $\bar{\tau}_{\text{pr}} = 0.327$, $\bar{\tau}_{\text{pr}} = 0.317$, or the proper flow radius of Wilson flow $\sqrt{8\tau} \approx 0.214$, 0.137 and 0.104 fm for the lattice ensemble 16^4 at $\beta = 4.5$, $24^3 \times 48$ at $\beta = 4.8$, and 32^4 at $\beta = 5.0$, respectively. This indicates that we can choose $\bar{\tau}_{\text{pr}}$ for gluonic $q_{\text{wf}}(x)$ to match with fermionic $q_{\text{smp}}(x)$.

All results show that Q_{wf} deviates largely from an integer for the proper flow time of Wilson flow fixed by the matching procedure. This phenomenon may be due to the fact that the topological charge is the global property of topological structure. However, the matching parameter Ξ_{AB} only shows the local matching property of topological charge density. Otherwise, the topological charge is the effect of the infrared properties, and the ultraviolet fluctuations lead to unphysical results as well as to non-integer topological charge values. Wilson flow is indeed a smoothing scheme of gauge fields. However, Wilson flow will modify the gauge field at the same time, which does not satisfy that the topological charge is conserved. In contrast, $F_{\mu\nu}^{\text{Imp}}$ in Eq. (14) is applicable under the classical expansion with respect to lattice spacing a , and it may be affected by some quantum fluctuations even though the smoothing is performed.

However, the topological charge is not the main quantity of interest, and the physically relevant observ-

able is the topological susceptibility. The results show that to make the topological charge close to an integer, larger Wilson flow time is required. It is noted that too large a Wilson flow time may wipe out the negative core of the topological charge density correlator [31]. However, the flow time for the topological susceptibility to reach a plateau is smaller than the flow time for the topological charges reach some integers [28]. Nonetheless, the topological susceptibility using the SMP method is too expensive to calculate. In future work, we may try to consider it.

In Fig. 3, Ξ_{AB} versus the flow time of Wilson flow of one configuration for lattices of 16^4 , $24^3 \times 48$, and 32^4 are shown. Ξ_{AB} for other configurations have a similar trend. We see that as the flow time of Wilson flow τ increases, Ξ_{AB} reaches a maximum value and then decreases. When the parameter κ is fixed, we can observe that as the lattice spacing decreases, the proper flow time of Wilson flow almost uniformly decreases, as expected. It also shows that as the lattice spacing a decreases, Ξ_{AB} tends to increase.

IV. CONCLUSIONS

We have analyzed the topological charge density $q(x)$ of all time slices using direct visualizations. We find that the SMP method is a good choice to study the topological charge density in the fermionic definition, and the SMP method is much cheaper than the traditional point source method, especially for a large lattice volume. The results show that the topological charge density depends on the Wilson mass parameter m in the fermionic definition. By comparing the $q_{\text{smp}}(x)$ with the gluonic definition of $q_{\text{wf}}(x)$, a correlation between m and τ is revealed. Smaller values of κ remove non-trivial topological charge fluctuations, which are similar to Wilson flow with a larger flow time. The detailed reasons are worthy of further study. By analyzing the topological charge density $q(x)$, we find that the proper flow time of Wilson flow for the gluonic definition of topological charge density can be obtained by the comparison of $q_{\text{smp}}(x)$ with $q_{\text{wf}}(x)$. We

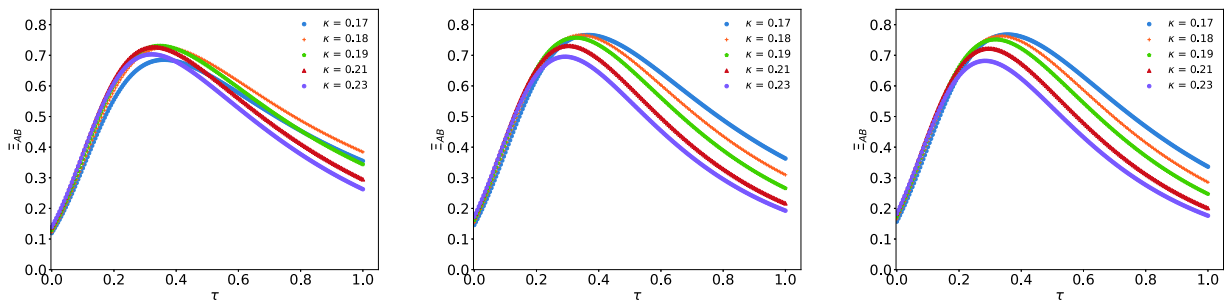


Fig. 3. (color online) Ξ_{AB} versus τ of one configuration for lattices of 16^4 , $24^3 \times 48$ and 32^4 . From left to right, the first figure is Ξ_{AB} versus τ for lattice volume 16^4 , the second figure for lattice volume $24^3 \times 48$, and the last one for lattice volume 32^4 . As κ is reduced, the proper flow time of Wilson flow is increased. As the lattice spacing decreases, Ξ_{AB} tends to increase.

also observe that the proper flow time of Wilson flow decreases with the decrease in lattice spacing a , which is consistent with expectations. Furthermore, as the lattice spacing a decreases, Ξ_{AB} tends to increase.

We also find that the topological charge obtained by Wilson flow at the proper flow time is far from an integer, and it is different from that of the fermionic definition. Although the topological charge density of the fermionic definition and that of the gluonic definition have the best match, the topological charge from the fermionic and gluonic definition are very different. The reason for this phenomenon may be that the matching parameter Ξ_{AB} only shows the local matching property of topological charge density, but the topological charge is the global property of topological structure. In contrast, Wilson flow can indeed smooth the gauge field. However, Wilson flow also changes the configurations, which does not guarantee the conservation of topological charge. Otherwise, in the gluonic definition of topological charge density, we used the improved field strength tensor corrected

in the classical expansion with respect to lattice spacing, which may be affected by the quantum fluctuations even though the Wilson flow is used. The detailed reasons need further study.

In the SMP method, we had known that the error is dependent on the off-diagonal components of the overlap operator. With a larger distance parameter, it has smaller errors in the SMP method. We can try to choose a larger distance parameter to decrease the error in future work. Otherwise, we could try to improve the field strength tensor to reduce the effect of classical expansion with respect to the lattice spacing in the gluonic definition of topological charge density.

ACKNOWLEDGMENTS

We are grateful to Heng-tong Ding for careful reading of the manuscript and useful suggestions. Numerical simulations have been performed on the Tianhe-2 supercomputer at the National Supercomputer Center in Guangzhou (NSCC-GZ), China.

References

- [1] G. Schierholz, Nucl. Phys. Proc. Suppl. **37A**, 203-210 (1994), arXiv:[hep-lat/9403012](#)
- [2] Edward Witten, Nucl. Phys. B **149**, 285-320 (1979)
- [3] Dmitri Diakonov, Proc. Int. Sch. Phys. Fermi **130**, 397-432 (1996), arXiv:[hep-ph/9602375](#)
- [4] Krzysztof Cichy, Arthur Dromard, Elena Garcia-Ramos *et al.*, PoS **LATTICE2014**, 075 (2014), arXiv:[1411.1205](#)
- [5] M. Müller-Preussker, PoS **LATTICE2014**, 003 (2015), arXiv:[1503.01254](#)
- [6] Constantia Alexandrou, Andreas Athenodorou, Krzysztof Cichy *et al.*, Eur. Phys. J. C **80**, 424 (2020), arXiv:[1708.00696](#)
- [7] M. F. Atiyah and I. M. Singer, Annals Math. **93**, 139-149 (1971)
- [8] Peter Hasenfratz, Victor Laliena, and Ferenc Niedermayer, Phys. Lett. B **427**, 125-131 (1998), arXiv:[hep-lat/9801021](#)
- [9] A. A. Belavin, Alexander M. Polyakov, A. S. Schwartz *et al.*, Phys. Lett. B **59**, 85-87 (1975)
- [10] Kazuo Fujikawa, Nucl. Phys. B **546**, 480-494 (1999)
- [11] Yoshio Kikukawa and Atsushi Yamada, Phys. Lett. B **448**, 265-274 (1999), arXiv:[hep-lat/9806013](#)
- [12] Herbert Neuberger, Phys. Lett. B **417**, 141-144 (1998), arXiv:[hep-lat/9707022](#)
- [13] Herbert Neuberger, Phys. Lett. B **427**, 353-355 (1998), arXiv:[hep-lat/9801031](#)
- [14] I. Horváth, S. J. Dong, Terrence Draper *et al.*, Phys. Rev. D **68**, 114505 (2003), arXiv:[hep-lat/0302009](#)
- [15] E.-M. Ilgenfritz, K. Koller, Y. Koma *et al.*, Phys. Rev. D **76**, 034506 (2007), arXiv:[0705.0018](#)
- [16] Guang-Yi Xiong, Jian-Bo Zhang, and You-Hao Zou, Chin. Phys. C **43**(3), 033102 (2019)
- [17] Rajamani Narayanan and Herbert Neuberger, Nucl. Phys. B **443**, 305-385 (1995), arXiv:[hep-th/9411108](#)
- [18] Robert G. Edwards, Urs M. Heller, and Rajamani Narayanan, Nucl. Phys. B **535**, 403-422 (1998), arXiv:[hep-lat/9802016](#)
- [19] Rajamani Narayanan and Pavlos M. Vranas, Nucl. Phys. B **506**, 373-386 (1997), arXiv:[hep-lat/9702005](#)
- [20] J. B. Zhang, S. O. Bilson-Thompson, F. D. R. Bonnet *et al.*, Phys. Rev. D **65**, 074510 (2002), arXiv:[hep-lat/0111060](#)
- [21] Hans Mathias Mamen Vege, *Solving SU(3) Yang-Mills theory on the lattice: a calculation of selected gauge observables with gradient flow*, Master's thesis (2019) U. Oslo (main)
- [22] Peter J. Moran, Derek B. Leinweber, and Jianbo Zhang, Phys. Lett. B **695**, 337-342 (2011), arXiv:[1007.0854](#)
- [23] M. Lüscher and P. Weisz, Commun. Math. Phys. **97**, 19 (1985) [Erratum: Commun. Math. Phys. **98**, 433 (1985)]
- [24] Frederic D. R. Bonnet, Derek B. Leinweber, Anthony G. Williams *et al.*, Phys. Rev. D **65**, 114510 (2002), arXiv:[hep-lat/0106023](#)
- [25] Zhen Cheng, Jian-Bo Zhang, and Guang-Yi Xiong, Chin. Phys. C **44**(3), 033104 (2020)
- [26] Martin Lüscher, JHEP **08**, 071 (2010) [Erratum: JHEP **03**, 092 (2014)], arXiv:[1006.4518](#)
- [27] Claudio Bonati and Massimo D'Elia, Phys. Rev. D **89**, 105005 (2014), arXiv:[1401.2441](#)
- [28] Constantia Alexandrou, Andreas Athenodorou, and Karl Jansen, Phys. Rev. D **92**, 125014 (2015), arXiv:[1509.04259](#)
- [29] Sundance O. Bilson-Thompson, Derek B. Leinweber, and Anthony G. Williams, Annals Phys. **304**, 1-21 (2003), arXiv:[hep-lat/0203008](#)
- [30] Falk Bruckmann, Christof Gattringer, Ernst-Michael Ilgenfritz *et al.*, Eur. Phys. J. A **33**, 333-338 (2007), arXiv:[hep-lat/0612024](#)
- [31] Abhishek Chowdhury, A. Harindranath, and Jyotirmoy Maiti, Phys. Rev. D **91**, 074507 (2015), arXiv:[1409.6459](#)